Anton HABJANIČ, Marko JESENIK, and Mladen TRLEP

University of Maribor, Faculty of Electrical Engineering and Computer Science

The advantages of the finite line elements application for the analysis of the grounding systems

Abstract. *In this paper, the new numerical model is presented to analyze the electromagnetic field around the grounding rod and grounding wire. In contrast to recently existent procedure based on the "classical" finite element method (FEM), in this new methodology the soil and the air domain of the problem are discretized by the 3-D finite elements and the conductors of the grounding electrodes are discretized by 1-D finite line elements. The results of calculations have been verified by comparison with the results of measurements found in the literature.*

Streszczenie. *W artykule prezentowane jest analiza pola elektromagnetycznego wokół pręta uziemiającego i obwodu uziemiającego. W przeciwieństwie do istniejących metod analizy, bazujących na metodzie elementów skończonych (MES) wprowadzono nową metodę, w której gleba i obszar powietrzny są dyskretyzowane siatką elementów skończonych 3-D a przewodniki uziemiających elektrod przez sieć elementów skończonych 1-D. Wyniki obliczeń skonfrontowano z wynikami pomiarów z literatury. (**Zalety zastosowania liniowych elementów skończonychdo analizy systemów uziemiających**)*

Keywords: electromagnetic transient analysis, finite element methods, grounding electrodes .
Słowa kluczowe: analiza elektromagnetycznych stanów przejściowych, metoda elementów skończonych, uziemiające elektrody

Introduction

The primary goal of grounding systems is to provide conductive paths to dissipate electrical currents into the ground, in order to ensure the safety of personnel and prevent damage of electrical installations, while their secondary goal is to provide common reference voltage for all interconnected electrical and electronic systems. To optimize the design of grounding systems, as well as to minimize the disturbance level in the protected area, the program tool able to analyze the transient performance of grounding systems is fundamental. For that very reason, the goal of this work was to develop the methodology (the proper numerical model) which allows a complete 3-D electromagnetic study of grounding systems by implying the finite line elements into the recently known numerical model of the transient electromagnetic field surrounding the grounding system based on the finite element method (FEM).

It is well known that the application of the "classical" FEM, where beside the soil and the air domain of the problem also the grounding system's conductors have to be discretized by the 3-D finite elements, is not sufficiently adapted for the grounding systems with thin structures. Therefore, in order to avoid numerical problems due to disproportionate dimensions of the grounding system's conductors, in this paper, the new numerical model is presented how to substitute the volume meshing of the thin conductors of the grounding rod and the grounding wire by the 1-D finite line elements discretization. The validity of the suggested method of grounding systems analysis has been verified by the results found in [1].

Numerical model of transient electromagnetic field based on FEM

The governing partial differential equation for quasi-static finite elements formulation of the electromagnetic field surrounding the grounding electrode can be derived from Maxwell's equations. In terms of the magnetic vector potential $\boldsymbol{A}$ and the electric scalar potential φ, it can be formulated as:

$$(1) \qquad \nabla\times\frac{1}{\mu}\nabla\times\boldsymbol{A}-\nabla\frac{1}{\mu}\nabla\boldsymbol{A}+\sigma\frac{\partial\boldsymbol{A}}{\partial t}+\sigma\nabla\varphi=0\,,$$

where μ is the permeability and σ the electrical conductivity.

By applying the finit elements procedure, the soil and air domain of the problem are discretized by the prismatic elements of the first order and the grounding electrodes are discretized by the line elements of the first order.

Thereby, the unknowns $\boldsymbol{A}$ and φ in arbitrary point along the finite line elements are approximated between the computed values of the corresponding potentials in the finite element's nodes (A_{xi}, A_{yi}, A_{zi}, and φ_{i}) in terms of interpolation functions (polynomials) N_{i} as:

$$(2) \quad \boldsymbol{A}=\sum_{i=1}^{2}\left(\overline{1}_{\mathrm{x}}A_{\mathrm{xi}}N_{\mathrm{i}}+\overline{1}_{\mathrm{y}}A_{\mathrm{yi}}N_{\mathrm{i}}+\overline{1}_{\mathrm{z}}A_{\mathrm{zi}}N_{\mathrm{i}}\right),\quad \varphi=\sum_{i=1}^{2}\varphi_{\mathrm{i}}N_{\mathrm{i}}\,.$$

Using the mathematical derivation described in [2] and [3], the final system of equations for the conductive domain of the problem, which consists of vectorial equation (3) and scalar equation (4), can be written:

$$(3) \int_{l}S\left[\frac{1}{\mu}\nabla\times\boldsymbol{N}_{\mathrm{i}}\nabla\times\boldsymbol{A}+\frac{1}{\mu}\nabla\boldsymbol{N}_{\mathrm{i}}\nabla\boldsymbol{A}+\sigma\boldsymbol{N}_{\mathrm{i}}\frac{\partial\boldsymbol{A}}{\partial t}+\sigma\boldsymbol{N}_{\mathrm{i}}\nabla\varphi\right]\mathrm{d}l=0\,,$$

$$(4) \qquad \int_{l}S\left[\nabla N_{\mathrm{i}}\,\sigma\frac{\partial\boldsymbol{A}}{\partial t}+\nabla N_{\mathrm{i}}\,\sigma\nabla\varphi\right]\mathrm{d}l=0\,.$$

To obtain the symmetry of the finite element's matrix and consequently the matrix of the system (as shown in (6)), the special modified electric scalar potential V is introduced as:

$$(5) \qquad \varphi=\frac{\partial V}{\partial t}=\dot{V}\,.$$

Regarding (5), the final matrix equation of the system for the finite line element in the conductive domain can be written as:

$$(6) \quad \begin{bmatrix}\mathbf{k}_{11}&\mathbf{k}_{12}&\mathbf{k}_{13}&0\\ \mathbf{k}_{21}&\mathbf{k}_{22}&\mathbf{k}_{23}&0\\ \mathbf{k}_{31}&\mathbf{k}_{32}&\mathbf{k}_{33}&0\\ 0&0&0&0\end{bmatrix}\cdot\begin{Bmatrix}\boldsymbol{A}_{\mathrm{x}}\\ \boldsymbol{A}_{\mathrm{y}}\\ \boldsymbol{A}_{\mathrm{z}}\\ \boldsymbol{V}\end{Bmatrix}+\begin{bmatrix}\mathbf{c}_{11}&0&0&\mathbf{c}_{14}\\ 0&\mathbf{c}_{22}&0&\mathbf{c}_{24}\\ 0&0&\mathbf{c}_{33}&\mathbf{c}_{34}\\ \mathbf{c}_{41}&\mathbf{c}_{42}&\mathbf{c}_{43}&\mathbf{c}_{44}\end{bmatrix}\cdot\begin{Bmatrix}\dot{\boldsymbol{A}}_{\mathrm{x}}\\ \dot{\boldsymbol{A}}_{\mathrm{y}}\\ \dot{\boldsymbol{A}}_{\mathrm{z}}\\ \dot{\boldsymbol{V}}\end{Bmatrix}=\begin{Bmatrix}0\\0\\0\\0\end{Bmatrix},$$

where **k** and **c** are the matrixes of dimension 2×2.

Vertical line element

Considering some fundamental mathematical relations presented in [3], for the vertical finite line element, where the potential is changing only along the *z* axis of the coordinate system, the particular coefficients of the finite line element's matrix equation (which are different from zero) can be expressed as:

(7) $$\mathbf{k}_{11ij} = \mathbf{k}_{22ij} = \mathbf{k}_{33ij} = S\int_l \left[\frac{1}{\mu}\frac{\partial N_i}{\partial z}\frac{\partial N_j}{\partial z}\right] dl ,$$

(8) $$\mathbf{c}_{11ij} = \mathbf{c}_{22ij} = \mathbf{c}_{33ij} = S\int_l \left[\sigma N_i N_j\right] dl ,$$

(9, 10) $$\mathbf{c}_{34ij} = S\int_l \left[\sigma N_i \frac{\partial N_j}{\partial z}\right] dl , \quad \mathbf{c}_{43ij} = S\int_l \left[\sigma \frac{\partial N_i}{\partial z} N_j\right] dl ,$$

(11) $$\mathbf{c}_{44ij} = S\int_l \left[\sigma \frac{\partial N_i}{\partial z}\frac{\partial N_j}{\partial z}\right] dl .$$

For the analytical calculation of the particular coefficients of the matrix equation (6), applying the transformation from the global into the local coordinate system, the following relation can be used:

(12) $$\int_z f(z)\,dz = -v\int_{-1}^{1} f^*(\tau)\,d\tau .$$

Consequently, the interpolation functions N_i are written as:

(13) $$N_1 = \frac{1-\tau}{2}, \quad N_2 = \frac{1+\tau}{2}, \quad \text{where } \tau = \frac{z_c - z}{v},$$

v represents the half of the finite line element's length, and z_c is the z coordinate of the central point of the line element.

Regarding (12) and (13), the following final forms of expressions (7-11) were derived:

(14) $$\mathbf{k}_{11ij} = \mathbf{k}_{22ij} = \mathbf{k}_{33ij} = \frac{S}{\mu v}\begin{bmatrix} -\frac{1}{2} & \frac{1}{2} \\ \frac{1}{2} & -\frac{1}{2} \end{bmatrix},$$

(15) $$\mathbf{c}_{11ij} = \mathbf{c}_{22ij} = \mathbf{c}_{33ij} = \sigma S v\begin{bmatrix} -\frac{2}{3} & -\frac{1}{3} \\ -\frac{1}{3} & -\frac{2}{3} \end{bmatrix},$$

(16, 17) $$\mathbf{c}_{34ij} = \sigma S\begin{bmatrix} -\frac{1}{2} & \frac{1}{2} \\ -\frac{1}{2} & \frac{1}{2} \end{bmatrix}, \quad \mathbf{c}_{43ij} = \sigma S\begin{bmatrix} -\frac{1}{2} & -\frac{1}{2} \\ \frac{1}{2} & \frac{1}{2} \end{bmatrix},$$

(18) $$\mathbf{c}_{44ij} = \frac{\sigma S}{v}\begin{bmatrix} -\frac{1}{2} & \frac{1}{2} \\ \frac{1}{2} & -\frac{1}{2} \end{bmatrix}.$$

Horizontal line element

For the horizontal finite line element, where the potential is changing only along the x axis of the coordinate system, the particular coefficients of the finite line element's matrix equation (which are different from zero) can be expressed as:

(19) $$\mathbf{k}_{11ij} = \mathbf{k}_{22ij} = \mathbf{k}_{33ij} = S\int_l \left[\frac{1}{\mu}\frac{\partial N_i}{\partial x}\frac{\partial N_j}{\partial x}\right] dl ,$$

(20) $$\mathbf{c}_{11ij} = \mathbf{c}_{22ij} = \mathbf{c}_{33ij} = S\int_l \left[\sigma N_i N_j\right] dl ,$$

(21, 22) $$\mathbf{c}_{14ij} = S\int_l \left[\sigma N_i \frac{\partial N_j}{\partial x}\right] dl , \quad \mathbf{c}_{41ij} = S\int_l \left[\sigma \frac{\partial N_i}{\partial x} N_j\right] dl ,$$

(23) $$\mathbf{c}_{44ij} = S\int_l \left[\sigma \frac{\partial N_i}{\partial x}\frac{\partial N_j}{\partial x}\right] dl .$$

By applying the variable x into (12), the interpolation functions N_i can be written as:

(24) $$N_1 = \frac{1+\tau}{2}, \quad N_2 = \frac{1-\tau}{2}, \quad \text{where } \tau = \frac{x_c - x}{v},$$

Consequently, the following final forms of coefficients (19-23) were derived:

(25) $$\mathbf{k}_{11ij} = \mathbf{k}_{22ij} = \mathbf{k}_{33ij} = \frac{S}{\mu v}\begin{bmatrix} -\frac{1}{2} & \frac{1}{2} \\ \frac{1}{2} & -\frac{1}{2} \end{bmatrix},$$

(26) $$\mathbf{c}_{11ij} = \mathbf{c}_{22ij} = \mathbf{c}_{33ij} = \sigma S v\begin{bmatrix} -\frac{2}{3} & -\frac{1}{3} \\ -\frac{1}{3} & -\frac{2}{3} \end{bmatrix},$$

(27, 28) $$\mathbf{c}_{14ij} = \sigma S\begin{bmatrix} \frac{1}{2} & -\frac{1}{2} \\ \frac{1}{2} & -\frac{1}{2} \end{bmatrix}, \quad \mathbf{c}_{41ij} = \sigma S\begin{bmatrix} \frac{1}{2} & \frac{1}{2} \\ -\frac{1}{2} & -\frac{1}{2} \end{bmatrix},$$

(29) $$\mathbf{c}_{44ij} = \frac{\sigma S}{v}\begin{bmatrix} -\frac{1}{2} & \frac{1}{2} \\ \frac{1}{2} & -\frac{1}{2} \end{bmatrix}.$$

Final form of the line element's matrix equation

For the time integration, the explicit Euler's method is used in which the derivative of the potential is substituted by the difference of the potentials, as follows:

(30) $$\dot{\boldsymbol{A}}^{(n)} = \frac{\boldsymbol{A}^{(n)} - \boldsymbol{A}^{(n-1)}}{\Delta t},$$

(31) $$\dot{V}^{(n)} = \frac{V^{(n)} - V^{(n-1)}}{\Delta t} = \varphi^{(n)} .$$

If we introduce (30) and (31) into (6), the following expression for the calculation of the potential in the new time step (n), depending on the preceding time step (n-1), is obtained:

(32) $$\left[K + \frac{C}{\Delta t}\right]\left\{\boldsymbol{A}^{(n)}, V^{(n)}\right\} = \left[\frac{C}{\Delta t}\right]\left\{\boldsymbol{A}^{(n-1)}, V^{(n-1)}\right\},$$

where {$\boldsymbol{A}$, V} is the column vector of the unknown nodal potentials; K is the stiffness matrix which is associated with the potentials $\boldsymbol{A}$ and V, and the Laplacian operator Δ; C is the damping matrix which represents the contribution of the induced current term $\sigma\,\partial\boldsymbol{A}/\partial t$ to the system.

In transient calculations, a new calculation of electromagnetic field in each time step Δt is needed. From (32), it is obvious that the calculation at the time step n depends on the results from the previous time step n-1. The duration period of the individual time steps can be constant over the whole calculation interval t_c or it can change from one time step to another time step. If the time step is constant, the system matrix does not change in individual time steps.

Implementation of the numerical model

The developed program for the 3-D calculation of transient electromagnetic field, which has been written in Fortran, consists of three modules: the pre-processor, the processor, and the post-processor. In the pre-processor, where first of all the 3-D mesh of prismatic finite elements of the first order is built by the automatic mesh generator [4],

also the geometrical and physical input data, as well as the injected potential function, are defined. According to the geometry of the grounding system's conductors, in the pre-processing stage also the mesh of finite line elements of the first order is added between the adequate nodes of the 3-D mesh of prismatic finite elements. In the processor, the transient calculation is carried out, as shown in Fig. 1.

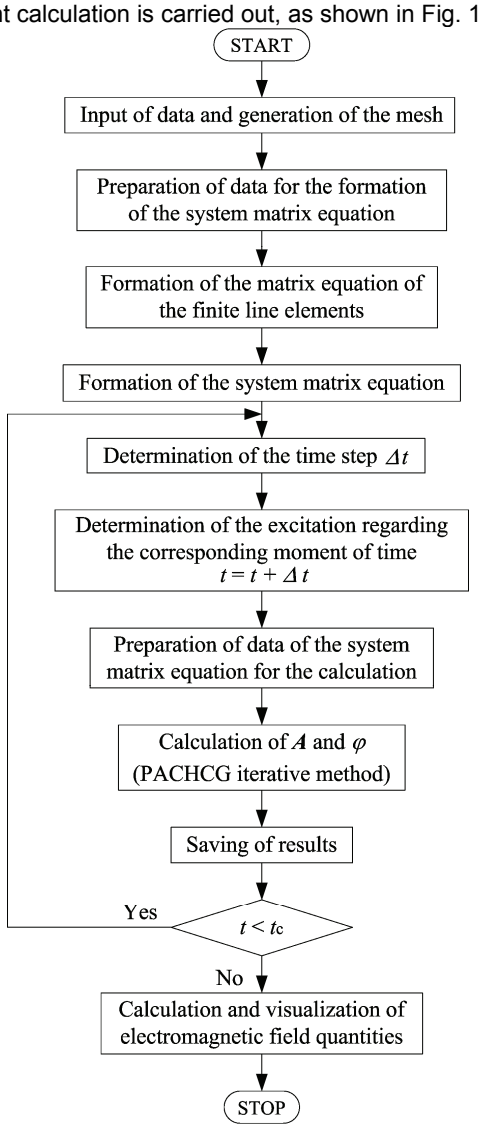

Fig.1. Flow chart of the electromagnetic transient calculation

To clearly indicate the form of finite element's matrix equation, in order to calculate the electromagnetic conditions in the particular region (material) of the analyzed problem, which is divided to the conductive and nonconductive region, let us again take into consideration the extended form of (6) for the finite elements forming the conductive region of the problem. Namely, in (6) the particular coefficients **k** and **c** represent the matrixes of dimension 6×6 into which the corresponding coefficients of the matrices of dimension 2×2, representing the adequate finite line element's equation, are already included. Whereas, the particular coefficients of the column vectors $\{\boldsymbol{A}, V\}$, $\{\dot{\boldsymbol{A}}, \dot{V}\}$ represent the vectors of dimension 6×1 into which the corresponding column vectors of dimension 2×1, representing the unknown potentials in the adequate finite line element's nodes, are also included.

Considering the marked areas in (6), which represent the extended form of the matrix equation for the finite elements forming the nonconductive region of the problem, one can conclude that, in comparison to the conductive region (e.g., ground or conductors of the grounding system) where both $\boldsymbol{A}$ and φ in all nodes of the discretized conductive domain are calculated, in the nonconductive region (air) all coefficients **c** are omitted, since they contain σ which is set to zero for the nonconductive materials. Consequently, (according to the $\boldsymbol{A}$, φ - $\boldsymbol{A}$ formulation of the problem [2]) just $\boldsymbol{A}$ in each node of the discretized nonconductive domain is calculated. In both cases, the set of derived linear algebraic equations is solved by the PACH conjugate gradient iterative method.

Finally, the post-processor allows interactive calculation and visualization of any desired quantity of electromagnetic field (e.g., current I, electric field intensity $\boldsymbol{E}$, magnetic flux density $\boldsymbol{B}$, etc.). Accordingly, once the components of $\boldsymbol{A}$ (A_x, A_y, A_z) and φ in all nodes of the discretized problem are known the electric current density $\boldsymbol{J}$ in arbitrary point in the soil surrounding the grounding system can be calculated by:

$$(33)\quad \boldsymbol{J} = -\sigma \frac{\partial \boldsymbol{A}}{\partial t} - \sigma \nabla \varphi \Rightarrow \begin{cases} J_x = -\sigma \dfrac{\left(A_x^{(n)} - A_x^{(n-1)}\right)}{\Delta t} - \sigma \dfrac{\partial \varphi^{(n)}}{\partial x} \\ J_y = -\sigma \dfrac{\left(A_y^{(n)} - A_y^{(n-1)}\right)}{\Delta t} - \sigma \dfrac{\partial \varphi^{(n)}}{\partial y} \\ J_z = -\sigma \dfrac{\left(A_z^{(n)} - A_z^{(n-1)}\right)}{\Delta t} - \sigma \dfrac{\partial \varphi^{(n)}}{\partial z} \end{cases}.$$

Since J_x, J_y, and J_z components of $\boldsymbol{J}$ are known, the absolute value of $\boldsymbol{J}$ can be obtained by:

$$(34)\quad |\boldsymbol{J}| = \sqrt{J_x^2 + J_y^2 + J_z^2}\ .$$

Finally, the current I that flows from the grounding system into the ground can be calculated by integrating over the arbitrary surface S that embraces the grounding system:

$$(35)\quad I = \int_S \boldsymbol{J}\,\mathrm{d}\boldsymbol{S} \doteq \sum_{i=1}^{n} J_n \Delta_e\ .$$

In (35), the number of finite elements composing S is denoted by n; J_n are the normal components of $\boldsymbol{J}$ throughout the S; and Δ_e are the surfaces of finite elements which coincide with S.

Application and discussion

Following up Geri's research work [1], concerning the development of the mathematical model based on a circuit approach, in this paper, the program solution is presented to analyze the transient behavior of the grounding rod and the grounding wire when fed by an injected potential function.

Vertical grounding rod simulation

The steel grounding rod with the length of 6 m, the diameter of 20 mm, and the conductivity of 5,88 × 10^6 S/m is buried vertically into the uniform soil with the resistivity of 40 Ω·m, as shown in Fig. 2, where also the defined boundary conditions on the outer planes of the problem are presented.

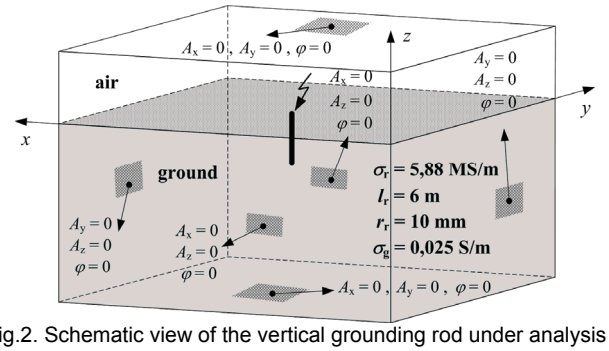

Fig.2. Schematic view of the vertical grounding rod under analysis

In order to verify the reliability of the program solution, in Fig. 3, the comparison of calculated current variations, obtained by the volume meshing (Current_FEM) and by the line discretization (Current_FEM_line) of the grounding rod as a response to the shape of the injected potential function, with current variation from [1] is presented.

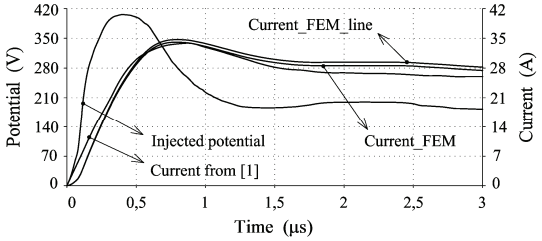

Fig.3. Comparison of the impulse response of the grounding rod

From the comparison of current variations in Fig. 3, the following statements can be made. First, the main cause of initial disagreement between the calculated results and the results from [1] is probably in the unreliable measured values of voltage obtained from [1] right after the beginning of surge current. Furthermore, some mistakes were also made by reading the current and voltage values in order to transfer the original current and voltage wave forms from [1] to Fig. 3. However, one can conclude that the model proposed in this paper is very effective and can be used to analyze the transient performance of grounding rods, as shown in Fig. 3.

Horizontal grounding wire simulation

With the intention to verify the application capability of the proposed methodology of grounding systems' modelling, the computer modelling has additionally been performed on the horizontally buried grounding wire. According to [1], a single copper wire with length of 15 m, the radius of 6 mm, and the conductivity of 58×10^6 S/m was analyzed. As show in Fig. 4, where also the defined boundary conditions on the outer planes of the problem are presented, the wire was placed horizontally at the depth of 0,6 m into the uniform soil with the resistivity of 70 Ω·m.

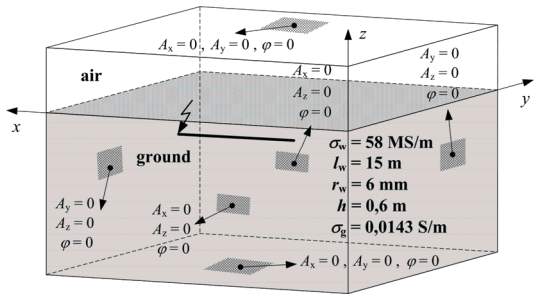

Fig.4. Schematic view of the analysed horizontal grounding wire

In Fig. 5, much "faster" wave form of injected potential into the grounding wire and consecutive current variations are shown in comparison to the case of grounding rod in Fig. 3. Also in this case, there are some disagreements between the computed current variations by the FEM and the current variation from [1]. Beside the same reasons as in case of the grounding rod, the main cause for the deviation of the results is probably in the disproportionate dimensions of the wire conductor ($r_w << l_w$) which must be discretized either by the 3-D finite elements or by the 1-D finite line elements. In this regard, the main reason for somewhat larger numerical mistakes and therefore considerably large initial difference between the calculated current variations (Current_FEM and Current_FEM_line) and the current variation from [1] originates from the steepness of the injected potential wave front which is very steep, as shown in Fig. 5.

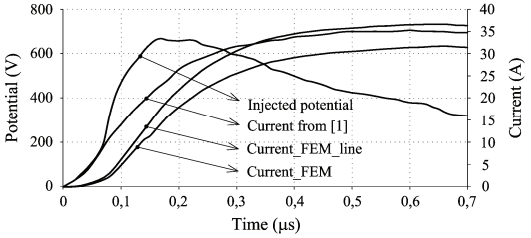

Fig.5. The transient voltage and currents of the grounding wire

However, the good agreement between the computed current variation (Current_ FEM_line) and the current variation from [1] shows the validity of our proposed method once again, and permits to confirm that our model simulates also the transient performance of horizontal grounding wires in a quite accurate way, as shown in Fig. 5.

Conclusion

The developed numerical model enables us to show the advantages of FEM modelling compared with the other methods traditionally used for this kind of problems. The main advantage lies in the ability to deal with the exact consideration of material's characteristics. Moreover, the soil constitution can be described in detail in every point in the area around the grounding system.

The results of the behavior analysis of the vertical grounding rod and the horizontal grounding wire, excited by the potential functions, in Fig. 3 and Fig. 5 respectively, show good agreement between the computed current variations and the current variation obtained from the literature, what also confirms the reliability of the proposed numerical model. And what is the most important, with the substitution of the volume meshing of the "thin" conductors by the line discretization, the calculation time is considerably reduced.

REFERENCES

[1] Geri A., Behaviour of grounding systems excited by high impulse currents: the model and its validation, *IEEE Transactions on Power Delivery*, vol. 14, no. 3, pp. 1008-1017, July 1999.

[2] Biro O. and Preis K., On the use of the magnetic vector potential in the finite element analysis of the three dimensional eddy current, *IEEE Transactions on Magnetics*, vol. 25, no. 4, pp. 3145-3159, July 1989.

[3] Habjanič A., *Numerical Model of Transient Electromagnetic Field around the Grounding System by the Finite Element Method*, Ph.D. dissertation, Faculty of Electrical Engineering and Computer Science, University of Maribor, Maribor, SLO, 2008, unpublished.

[4] Jesenik M., Trlep M., and Hribernik B., Algorithm for automatic 2D discretization with variable mesh density for numerical methods, *in Proceedings of 6th International IGTE Symposium*, Graz, pp. 132-137, September 1994.

[5] Nekhoul B., Labie P., Zgainski F. X., and Meunier G., Calculating the impedance of a grounding system, *IEEE Trans. on Magnetics*, vol. 32, no. 3, pp. 1509-1512, May 1996.

[6] Trlep M., Hamler A., and Hribernik B., The analysis of complex grounding systems by FEM, *IEEE Transactions on Magnetics*, vol. 34, pp. 2521-2524, September 1998.

[7] Habjanič A., Trlep M., The simulation of the soil ionization phenomenon around the grounding system by the FEM, *IEEE Trans. on Magnetics*, vol. 42, no. 4, pp. 867-870, April 2006.

***Authors**: Anton Habjanič, Ph.D., University of Maribor, E-mail: anton.habjanic@uni-mb.si; prof. Mladen Trlep, E-mail: mladen.trlep@uni-mb.si*

Marko Jesenik, Ph.D., E-mail: marko.jesenik@uni-mb.si

University of Maribor, Faculty of Electrical Engineering and Computer Science, Smetanova ul. 17, 2000 Maribor.